

Connection between interannual variability of the western Pacific and eastern Indian Oceans in the 1997~1998 El Niño event*

WANG Dongxiao**, LIU Qinyan, LIU Yun and SHI Ping

(LED, South China Sea Institute of Oceanology, Chinese Academy of Sciences, Guangzhou 510301, China)

Received August 4, 2003; revised August 28, 2003

Abstract In this paper, the sea surface height and the heat content of the upper ocean are analyzed to retrieve the relationship of interannual variabilities between the tropical western Pacific and eastern Indian Oceans during the 1997~1998 El Niño event. In the prophase of this El Niño, the negative sea level anomalies (SLA) occurred in the tropical western Pacific (TWP) firstly, and then appeared in the tropical eastern Indian Ocean (TEI). The negative heat content anomalies (HCA) emerged in the TWP before this El Niño burst while the SLA signals developed over there. During the mature stage of this El Niño, two kinds of signals in the TWP and TEI turned to be the maximum negative sequently. Due to the connected interannual adjustment between the TEI and TWP, we adopted a method to estimate the Indonesian Throughflow (ITF) transport by calculating the HCA budget in the TEI. The indirect estimation of the ITF was comparable to the observation values. Therefore, the anomalies in the TEI had been proved as advecting from the TWP through the ITF during the 1997~1998 El Niño.

Keywords: Indonesian Throughflow, El Niño, tropical East Indian Ocean.

Some evidence of possible connections between the tropical western Pacific (TWP) and tropical eastern Indian (TEI) Oceans on the interannual timescales were reported^[1-3]. Tourre et al.^[4] investigated the interannual relationship for the heat content anomalies (HCA) in both the Pacific and Indian Oceans during the 1983~1987 El Niño periods. They found that the anomalous signals in the Indian Ocean lagged the El Niño event by about 6 months in 1983, whereas they were in accordance with the event in 1987.

About the physical mechanism of the inter-basin connection between the Pacific and Indian Oceans, there are different interpretations, such as the atmosphere-ocean interaction, the atmospheric tele-connection, and the ocean internal linkage. Latif et al.^[5] studied the interannual signals of three tropical ocean basins. They pointed out that sea surface temperature (SST) anomalies in the tropical Pacific can excite the local atmospheric anomalies. These signals then transferred to the tropical Indian Ocean loaded by the Walker circulation, resulting in the interannual variation in the tropical Indian Ocean via a local ocean-atmosphere interaction. The implied meaning of this point is that there is a zonal atmospheric bridge

over the two ocean regions. Wu et al.^[6] revealed that there is a positive correlation dominantly on the interannual timescale between the equatorial Pacific and eastern Indian Oceans. The coupling mechanism is caused by these two Walker circulations that work in a way much like a pair of gears operating over the equatorial Indian and Pacific Oceans. Webster et al.^[7] and Saji et al.^[8] did some dynamic analyses about the Indian Ocean warm event, and they disproved that this warm event has any solid connection with the upper layer variability in the Pacific. But Li et al.^[9] pointed out the existence of a certain relation between the Indian Ocean dipole events and SST anomalies in the Pacific.

It is well known that the Indonesian seas provide a low-latitude pathway for the transfer of warm, low salinity Pacific waters into the Indian Ocean. The ITF is the main transport way linking the Pacific with Indian Oceans. Therefore, the ITF and its variability have important influences on heat content in the Pacific warm pool and on the TEI circulation pattern. Some previous researches have demonstrated that the ITF is one of the ways connecting the seasonal to interannual variabilities in these two tropical ocean basins^[2,3].

* Supported by the National Natural Science Foundation of China (Grant Nos. 40136010 and 40028605) and the Chinese Academy of Sciences (Grant No. KZCX2-205)

** To whom correspondence should be addressed. E-mail: dxwang@scsio.ac.cn

This paper focuses on the relationship of the interannual signals both in the TWP and TEI during the 1997~1998 El Niño event, the strongest one in the last century. In order to explore the most possible role played by the ITF, as an ideal precondition, we ignore the effect on interannual variability in the TWP and TEI carried by the atmospheric bridge.

1 Data and methods

The altimeter remote sensed sea level data from 1992 to 1998 we used are provided by Collecte Localisation Satellites (CLS), France, and the monthly re-analyzed wind fields are supplied by National Centers for Environmental Prediction/National Center of Atmospheric Research (NCEP/NCAR), USA. Temperatures at several standard depths from the surface to 400 m consist of all available expendable bathythermograph (XBT) data over the 1955~1999 period assembled and quality controlled by the Scripps Joint Environmental Data Analysis Center^[10]. We calculate the heat content from the surface to the 20 °C isotherm depth:

$$Q = S \int_{-h}^0 \rho C_p T dz, \quad (1)$$

where S is the grid unit area of the 5° longitude by 2° latitude resolution, C_p the constant pressure specific heat, h the 20 °C isotherm depth (obtained from interpolation over the standard levels). Simply, we define $S\rho C_p = 1$ (relative unit). The HCA in the upper layer was gotten by subtracting the 20-year averaged climatology from 1980 to 1999. Some monthly mean was converted to seasonal mean. Here spring is from March to May, and summer is from June to August, and fall is from September to November, and winter is from December to February of the next year.

2 Interannual variability in SLA and HCA

Plate I shows several seasonal mean SLA in the study domain of the TWP and TEI. The SLA is positive in the summer of 1996 (Plate I(a)), and is stronger in the fall of 1996 (Plate I(b)), which are also noticed by Chambers et al.^[3] and Potemra et al.^[14]. Regarding the HCA of the upper layer defined above, the similar phenomenon also occurs. That is to say, in both regions of the TWP and TEI, there are strong positive signals in the HCA during the summer (Fig. 1 (a)) and fall of 1996 (Fig. 1 (b)). The characteristics of SLA and HCA are shown here. The strong signals in the western Pacific are located north of the equator, whereas the strong

signals in the TEI lie in the equator and south of the equator.

Associated with the El Niño burst, the western Pacific warm pool extends eastward. In the spring of 1997, the SLA and HCA are both negative in the north of the equator in the far western Pacific (Plate I (c), Fig. 1(c)). At the same time, the positive SLA in the TEI relaxes. Though some positive anomalies also exist south of the equator off Australia, the negative anomalies occur in the equator and north of the equator. There is a similar scenario of variability in the HCA in these regions. The characteristic of HCA is not so clear because of the rough resolution.

In the summer of 1997, the SLA and HCA in the far western Pacific are both negative, and extend eastward and southward as a larger coverage. The negative anomalies are also dominant in the TEI (see Plate I(d), Fig. 1 (d)). These negative anomalies remain till the winter of 1997 (Plate I(e), Fig. 1 (e)). In the spring of 1998 (Plate I(f), Fig. 1 (f)), with the burst of El Niño, the negative anomalies begin to weaken. In the summer of 1998, there are positive anomalies for both SLA and HCA developing simultaneously in the TEI, as well as north of the equator of the TWP (figures omitted).

Analysis of the interannual variability in the studied domain presented above strongly suggests that there is a certain relationship between the SLA and HCA adjustments in the TWP and TEI Oceans, e.g. they are in accordance with each other in view of the large-scale evolution in the two regions. In addition, differences of these signals can also be seen here. The anomalies of the TWP are of earlier onset and stronger than those of the TEI.

For the purpose of clarifying the differences of signals, we choose two boxes with intensive signatures in the TEI and TWP, respectively. One of them (125° E ~ 145° E, 0° ~ 10° N) represents the SLA region north of the equator in the TWP. The other (100° E ~ 115° E, 20° S ~ 10° S) represents the SLA region in the TEI. Fig. 2 displays time series of those area-averaged HCAs, as well as their difference during 1992 ~ 1998. It can be clearly seen that the HCA in the TWP is earlier and stronger than that in the TEI during the 1997~1998 El Niño. The amplitude of SLA in the TEI is weaker than the TWP (figures omitted), and the amplitude of HCA in the TEI is about one-third of that in the TWP (see Fig. 2).

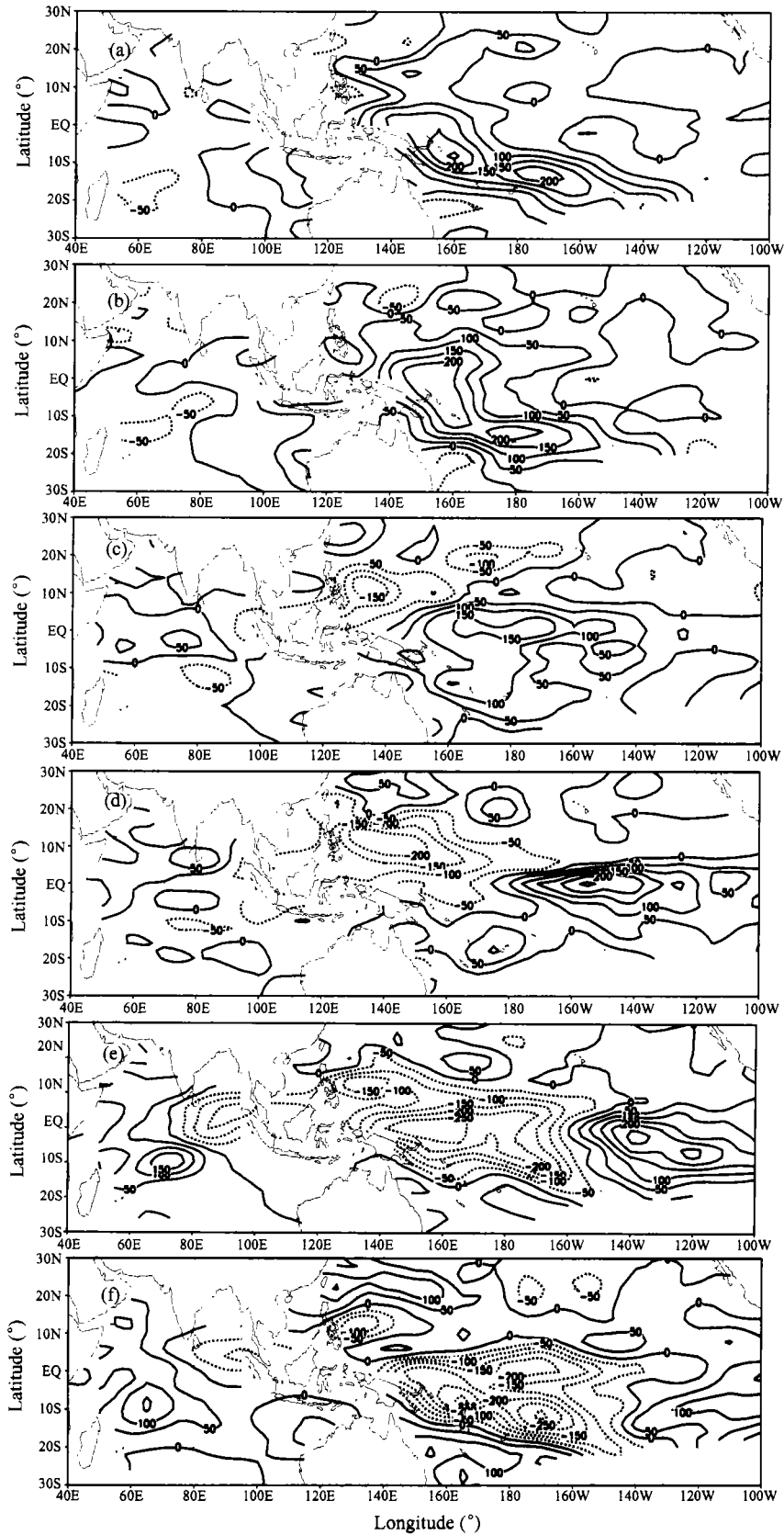


Fig. 1. Distribution of seasonal mean HCA above the thermocline depth. (a) Summer of 1996; (b) fall of 1996; (c) spring of 1997; (d) summer of 1997; (e) winter of 1997; (f) spring of 1998 (Unit: $10^7 \text{ W}\cdot\text{s}/\text{m}^2$, contour interval: 50).

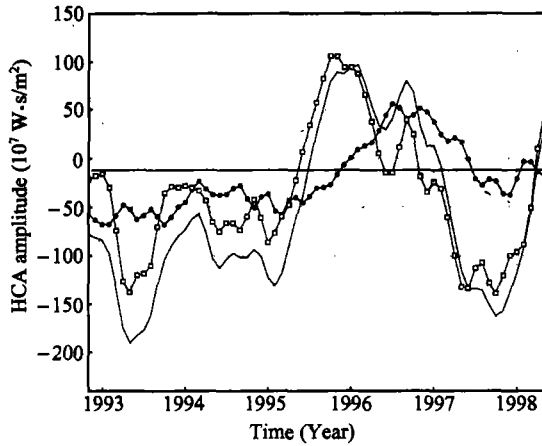


Fig. 2. Time series for the area-averaged HCA in Box 1 ($125^{\circ}\text{E} \sim 145^{\circ}\text{E}$, $0^{\circ} \sim 10^{\circ}\text{N}$) and Box 2 ($100^{\circ}\text{E} \sim 115^{\circ}\text{E}$, $20^{\circ}\text{S} \sim 10^{\circ}\text{S}$) with 9 points running mean, and their difference (Unit: $10^7 \text{ W}\cdot\text{s}/\text{m}^2$), solid line: Box 1, closed circle line: Box 2; open square line: their difference (Box 1 minus Box 2).

The wind forcing can influence the SLA variability in the Pacific and Indian Oceans. And the SLA changes also can imply the ITF variability because the ITF is fed by sea level gradient between the Pacific and Indian Oceans^[11]. Meyers^[1] and Gordon et al.^[12] found that the ITF transport during El Niño is less than in normal year. The SLA differences of the two boxes during the 1997~1998 El Niño are negative here (figure omitted, however, it can be inferred from the HCA difference in Fig. 2). The negative anomalies reflect indirectly the reduced ITF transport during the 1997~1998 El Niño.

In the summer of 1996, there are the easterly anomalies in the tropical Pacific, and the westerly anomalies in the TEI. Driven by the easterly anomalies (Fig. 3(a)), more warm water accumulates in the TWP than normal, and it favors sea-level rise,

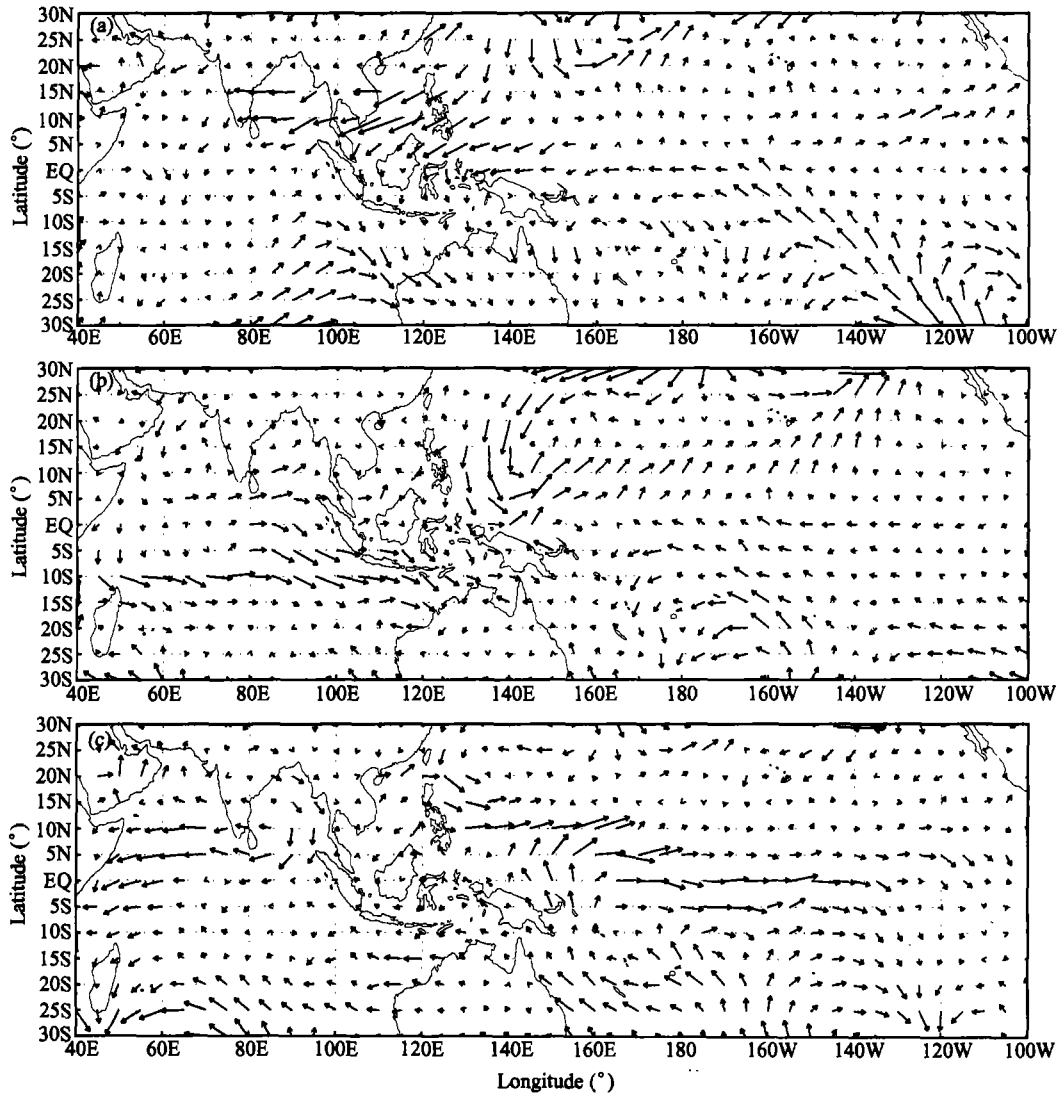


Fig. 3. Seasonal mean surface wind fields deriving from NECP reanalysis. (a) Anomalies in summer of 1996; (b) winter of 1996; (c) summer of 1997.

accompanied by enhanced heat content. Therefore, the SLA (Plate I(a)) and HCA (Fig. 1(a)) are both positive in the TWP at that time.

In the winter of 1996, the westerly burst occurred in the TWP, but the westerly anomalies also remained in the TEI (see Fig. 3(b)). Note that this pattern is against the "gear coupled" structure. In the summer of 1997 (see Fig. 3(c)), the wind anomalies changed as westerly in the TWP, and easterly in the TEI.

There is no evident feature in the wind field patterns in the TEI and TWP that supports the so-called "gear coupled" mechanism working in 1997~1998. One reason for its absence is that the "gear coupled" characteristic is statistically derived. Wu et al.^[6] analyzed the time series of zonal average wind in the Indian Ocean and Pacific region instead of verifying the horizontal large-scale wind fields, which we show here. The other reason is that their analyses do not include the 1997~1998 period. So whether the "gear coupled" mechanism worked in the 1997~1998 El Niño is to be determined.

A hypothesis that the ITF plays an important role is proposed here to explain the relationship of interannual variabilities in the TWP and TEI Oceans when two facts are concerned. First, there is a phase lag between occurrence of oceanic signals in the TWP and TEI Oceans. Second, the atmospheric bridge, which was proposed previously to interpret the coherent interannual variabilities in the two basins, did not work well during the 1997~1998 El Niño.

Therefore, in our hypothesis, the anomalies in the TEI are supposed to come from the TWP through the ITF. Based on the law of heat content balance, we can estimate the ITF indirectly. By comparing the estimation with observation of the ITF transport, one may make sure if the ITF can link those anomalies in the TWP and TEI or not.

3 Indirect estimation of the ITF transport

Observations and models indicate that the primary ITF source is North Pacific thermocline water flowing through the Makassar Strait. It is in agreement with the region where the SLA and HCA are apparent in the TWP. Given the HCA in the TEI are transferred by the ITF from the TWP, we can estimate the mean ITF transport according to increment of the HCA in the TEI within a certain period.

The area-averaged time series during the 1980~1999 period are constructed for the HCA in a box (125°E~145°E, 0°~10°N), north of the equator of the TWP, where the ITF origin is located (Fig. 4(a)). As a reference, correlation coefficients are calculated between the time series and those in each grid within the studied domain, while more attention is paid to correlation coefficient in the TEI (Fig. 4(b)). When the correlation coefficient is 0.3 (roughly above 95% confidence level), we choose the region in the TEI where the coefficient is larger than 0.3, and integrate the HCA to describe the evolution of interannual variability in the TEI (Fig. 4(c)). We select the region in the TEI where the correlation coefficients of the HCA referring to interannual variability in the TWP are larger than 0.3. This statistically derived region is regarded as the domain where the HCA variability is significantly affected by the influence of the western Pacific warm pool, meaning that both local surface heating and oceanic adjustment in the TEI contribute very little. This TWP-dependent area is similar to that depicted by Potemera et al.^[13] who revealed the first interannual mode of altimeter data in the western Pacific and eastern Indian Oceans. The time series of the integrated HCA over the TWP-dependent area showed that, when the 1997~1998 El Niño is concerned, the negative HCA occurred at the beginning of April 1997 (Fig. 4(c)). The negative HCA reached its maximum in November 1997, meaning that it took about 8 months for a mature signal to build up in the TEI. The averaged negative HCA in the ITF origin location over those 8 months, H_s , is -120.4 relative unit (Fig. 4(a)).

The maximum of HCA of the TWP-dependent area in the TEI is $H(-3.2 \times 10^3$ relative unit, see Fig. 4(c)). It is the accumulated result for the HCA transferred by the ITF from the TWP over about 8 months. The relationship describing the heat content balance can be expressed as

$$\begin{aligned} Q_1 &= \rho \cdot V \cdot C_p \cdot T' \cdot t, \\ Q &= H \cdot \rho \cdot C_p \cdot S, \end{aligned} \quad (2)$$

where Q_1 is the HCA transferred by the ITF, T' the area-averaged SST anomaly in the ITF origin, V the ITF transport, Q the increment of HCA in the Indian Ocean, and t the accumulating time that a mature HCA builds up in the TEI, i.e. 8 months. And ρ is the density of seawater, S area of the 5°-longitude by 2°-latitude grid, $T' = H_s/h$, h is the mean thermocline depth in the TWP-dependent area in the Indian Ocean (judged as the correlation coefficient larger

than 0.3 in Fig. 4(b)). Here it is 120 m, in agreement with the observation.

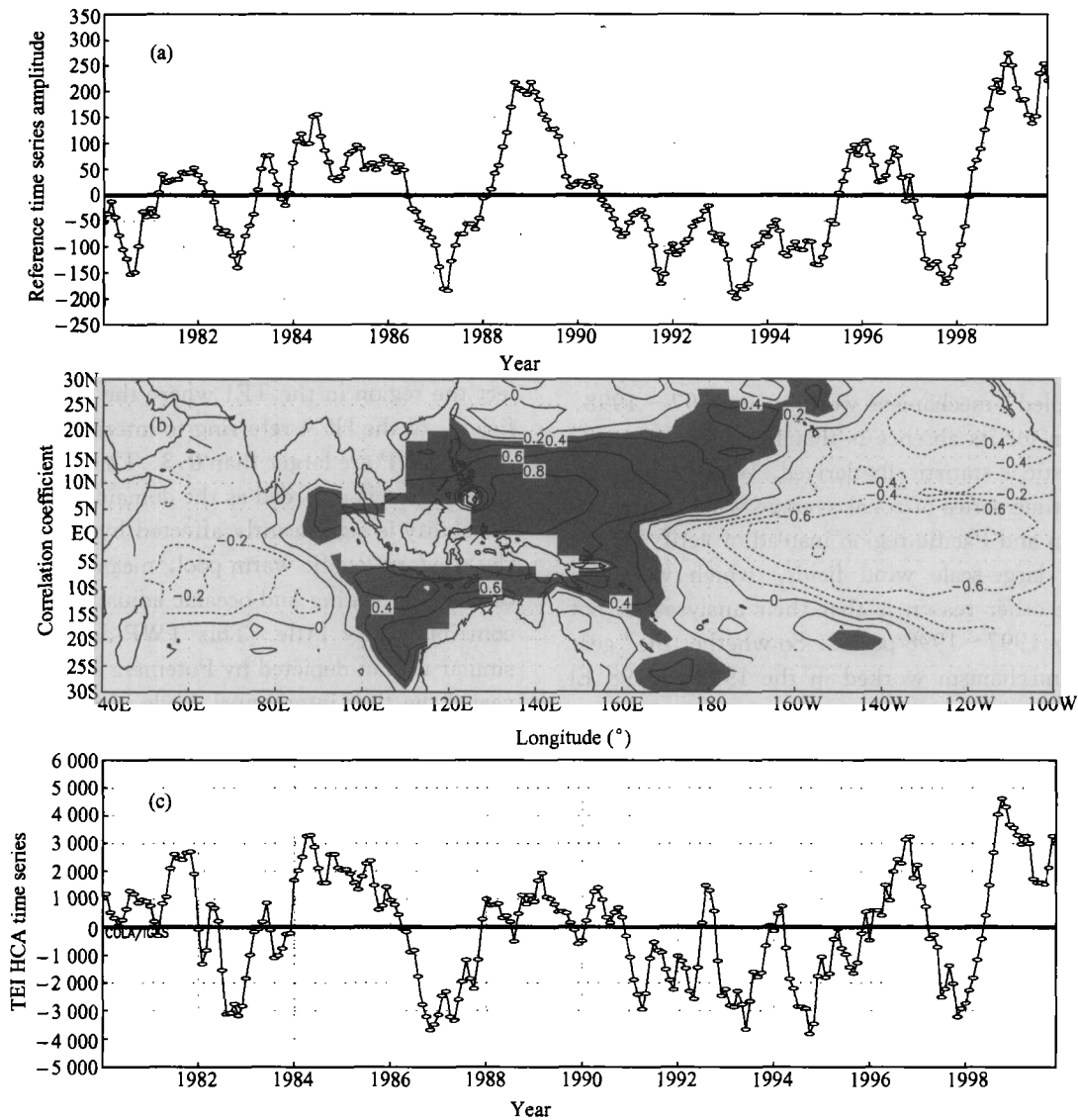


Fig. 4. Reference time series, HCA correlation coefficient and time series for the HCA integrated over the TWP-dependent region in the TEI. (a) Area-averaged time series for the HCA in Box 1 (125°E~145°E, 0°~10°N) in the 1980~1999 period, as the reference time series (Unit: $10^7 \text{ W}\cdot\text{s}/\text{m}^2$). (b) Distribution of the correlation coefficient between the HCA in the study domain and the reference time series (correlation coefficients larger than 0.3 are shaded). (c) Area-integrated time series for HCA in the TEI where correlation coefficients are larger than 0.3 (Unit: $10^7 \text{ W}\cdot\text{s}/\text{m}^2$).

According to the assumption, the HCA in the TEI is completely transferred by the ITF from the TWP without any local heating:

$$Q_I = Q. \quad (3)$$

So,

$$V = \frac{H \cdot S \cdot h}{H_s \cdot t}. \quad (4)$$

The ITF transport estimated here from the HCA budget is $19.0 S_v$ ($1 S_v = 10^6 \text{ m}^3/\text{s}$). The values of

observation and numerical simulation of the ITF transport vary from 0 to $30 S_v$. For example, Lebedev et al.^[14] diagnosed the mean ITF transport as $(11.5 \pm 1.1) S_v$ by using Levitus temperature, salinity and wind data. The value we estimated is not beyond the bound of this extension. Thus, it proves our hypothesis that the ITF transport has a certain contribution to establishment of the negative HCA in the TEI during the 1997~1998 El Niño.

4 Summary

Remote sensed sea level and XBT-derived heat content (i. e. SLA and HCA) are analyzed to retrieve the oceanic connecting relationship of interannual variabilities in the western Pacific and eastern Indian Oceans during 1997 ~ 1998 El Niño. Results show that SLA and HCA in the TWP and TEI bear similar developing phases. At the stage prior to the 1997 ~ 1998 El Niño burst, the anomalous westerly wind in the western Pacific drives a negative SLA and HCA in the TWP. The same sign SLA and HCA develop gradually in the TEI. It seems that the “gear coupled” mechanism does not work, in contrast to the previous El Niño events, when surface wind anomalies are highlighted here.

Based on a hypothesis that the thermal anomalies in the TEI are completely advected from the TWP, we estimate the ITF transport indirectly with respect to the heat content balance. A reasonable value in agreement with the observation is obtained. This indicates that the ITF transport can link the TWP and TEI Oceans on interannual time scale. The SLA and HCA of those two regions bear similar interannual variability during the 1997 ~ 1998 strong El Niño at least partly due to the ITF transport, in addition to the intrinsic atmospheric bridge.

References

- 1 Meyers, G. Variation of the Indonesian throughflow and the El Niño-Southern Oscillation. *J. Geophys. Res.*, 1996, 101: 12255.
- 2 Wang, D. et al. Oceanic thermal variability on the interannual timescale in the tropical Indian Ocean. In: *Proceedings of International Conference on Monsoon and Hydrologic Cycle*. 22~25 April 1998, Korean Meteorological Society, Kyongju, Korea, 179 ~ 188.
- 3 Chambers, D. P. et al. Anomalous warming in the Indian Ocean coincident with El Niño. *J. Geophys. Res.*, 1999, 104 (C2): 3035.
- 4 Tourre, Y. M. et al. El Niño signals in the global upper-ocean temperature. *J. Phys. Oceanogr.*, 1995, 25: 1317.
- 5 Latif, M. et al. Interactions of the tropical oceans. *J. Climate*, 1995, 8(4): 952.
- 6 Wu, G. et al. The gear couple and ENSO events of the atmosphere-ocean system between the equatorial Indian Ocean and Pacific Ocean I: data analysis. *Chin. J. of Atmos. Sci.* (in Chinese), 1998, 22(4): 470.
- 7 Webster, P. J. et al. Coupled ocean- atmosphere dynamics in the Indian Ocean during 1997~1998. *Nature*, 1999, 401: 356.
- 8 Saji, N. H. et al. A dipole mode in the tropical Indian Ocean. *Nature*, 1999, 401: 360.
- 9 Li, C. et al. Indian Ocean temperature dipole and SSTA in the equatorial Pacific Ocean. *Chinese Science Bulletin*, 2002, 47(3): 236.
- 10 White, W. B. Design of a global observing system for gyre-scale upper ocean temperature variability. *Progress in Oceanography*, 1995, 36: 169.
- 11 Meyers, G. et al., Geostrophic transport of Indonesian flow. *Deep Sea Res.*, Part I. 1995, 42: 1163.
- 12 Gordon, A L, et al. Pathways of water between the Pacific and Indian Oceans in the Indonesian seas. *Nature*, 1996, 379: 146.
- 13 Lebedev, K. V. et al. A diagnostic study of the Indonesian Throughflow. *J. Geophys. Res.*, 2000, 105: 11243.
- 14 Potemra, J. T. et al. Seasonal to interannual modes of sea level variability in the western Pacific and eastern Indian Oceans. *Geophys. Res. Lett.*, 1999, 26(3): 365.

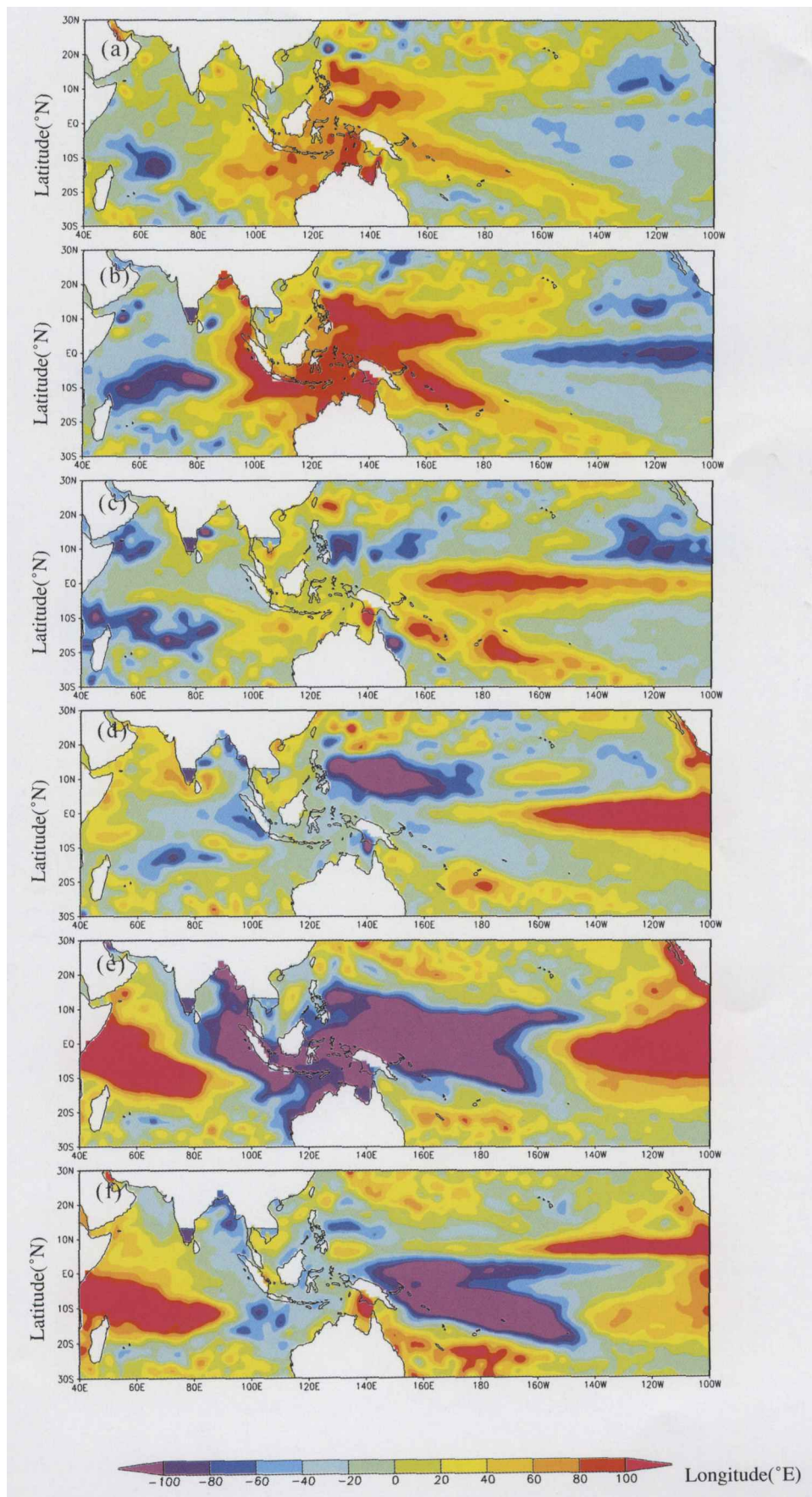


Plate I . Distribution of the seasonal mean SLA